

Antialiasing of Bump-Maps

Andreas G. Schilling

ISSN 0946-3852

WSI-97-15

Wilhelm-Schickard-Institut für Informatik

Graphisch-Interaktive Systeme

Auf der Morgenstelle 10/C9

D-72076 Tübingen

Tel.: +49 7071 29-75462

Fax: +49 7071 29-5466

email: schilling@uni-tuebingen.de

URL: <http://www.gris.uni-tuebingen.de/~andreas>

© copyright 1997 by WSI-GRIS
printed in Germany

Abstract

Bump-maps, like texture maps or any other maps consisting of discretely stored data have to be properly filtered, if they are being resampled in the process of rendering an image. If, however, bump maps are filtered in the traditional way, the bumps are lost in the filtering process and the result is a smooth surface. We introduce a bump map pyramid, that contains and preserves isotropic or anisotropic roughness information in all resolution levels.

Problem

The antialiasing of bump maps is similarly important as the antialiasing of textures in general (Fig. 1). However, filtering bump maps in the common way doesn't lead to the desired result, but instead results in a smoothed surface. The lower the resolution gets, the more we have to filter, the larger are the bumps that disappear (Fig. 2). So *filtering bump maps means to remove the bumps*. In reality however, a bumpy surface can be told from a smooth surface, even if it is viewed from a larger distance, where the individual bumps are not discernible anymore (Fig. 3). What can be seen in this case, is the bumpiness or roughness of the surface. The problem is, that filtering removes not only the individual bumps, but also the bumpiness. Bump maps can be represented as height- or offset-maps [4]. We prefer a representation that uses a two-dimensional vector field of offset vectors to be added to the normal vector, which is described below. But regardless of how a bump map is represented, filtering or averaging always leads to the mentioned effects.

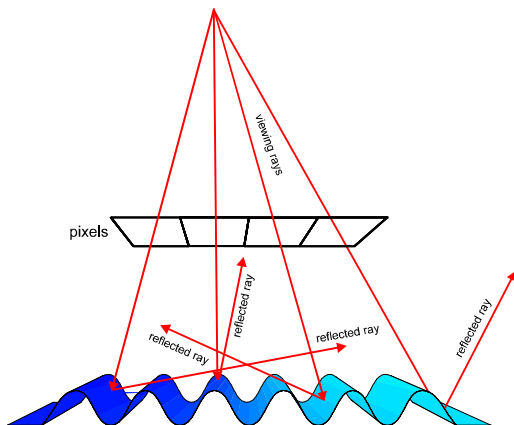


Fig. 1: Antialiasing of bump maps is necessary; otherwise we get rays reflected into random directions or random Phong illumination values.

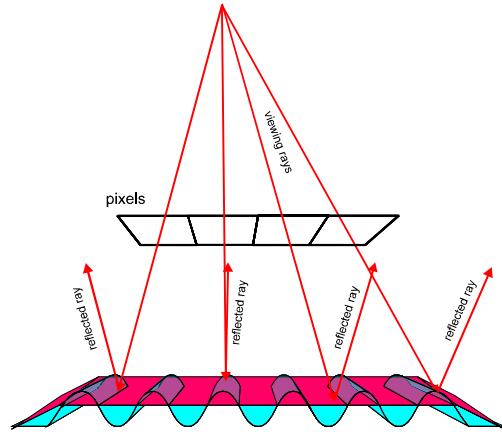


Fig. 2: Filtering the bump map removes bumps and produces a smooth surface

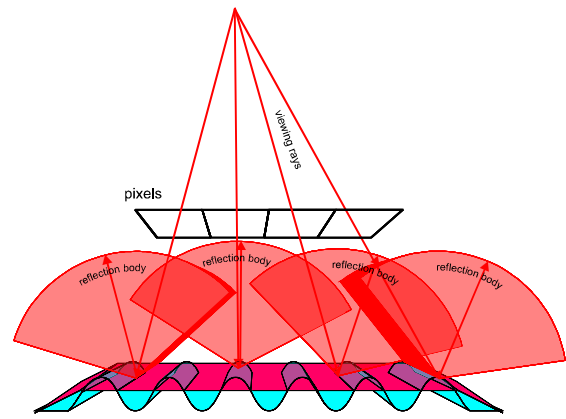


Fig. 3: The roughness of a surface causes rays from more than only one direction to be reflected into one pixel. These rays form a reflection cone or a conical reflection body

Related Work

Becker and Max [1] address the problem of rendering bump mapped surfaces in multiple resolutions. They switch between unfiltered bump maps and a BRDF (bi-directional reflection distribution function). In order to avoid inconsistencies between the two models, they use different redistribution functions for each viewing angle to modify the standard bump mapping. For a smooth transition, they blend between the results of the two algorithms. The use of the BRDF is the correct solution for rendering bumps that are too small to be discernible at a given resolution; however, the method is very expensive. In addition, it works only for bump maps containing only a narrow range of frequencies. Only in this case, a single transition point between bump mapping and using a BRDF can be determined. Therefore, bump maps containing a broader range of bump

frequencies have to be broken up into multiple maps, each limited to a narrow frequency range.

In his cone-tracing paper [5], Kirk uses cones instead of simple rays for the purpose of antialiasing. He even mentions the application for bump mapping, although he does not account for the roughness but only for the curvature of the surface (difference between normal vectors at the cone centerline intersection and the cone edge). In this paper, we use reflection bodies that could be regarded as a generalization of Kirk's cones to understand and describe the antialiasing of bump-maps.

A new Solution

If we want to preserve the important surface properties, in addition to the bump map we have to introduce and use a new type of maps: the roughness map. It stores the variance of the normal directions from the area that contributes to one sample in the filtered version of the bump map. Consider for example a lake, seen from some distance. Even if there are waves, the surface of the water within one pixels region can be represented by only one normal vector, if standard bump mapping is used. If this pixel region is large enough, this average normal vector will always point straight up. So we will get the same reflections of the sun (or any environment) as in a perfect mirror, regardless of the presence or absence of small waves. If we store, however, the roughness of the surface, we can account for the waves and get a better approximation of the lake than a perfect mirror would be. We could use the roughness as a measure for the exponent in the Blinn-Phong model[3]. A better way is described in [7], where environment maps are used and the roughness serves as a parameter for the anisotropic antialiasing of the environment map.

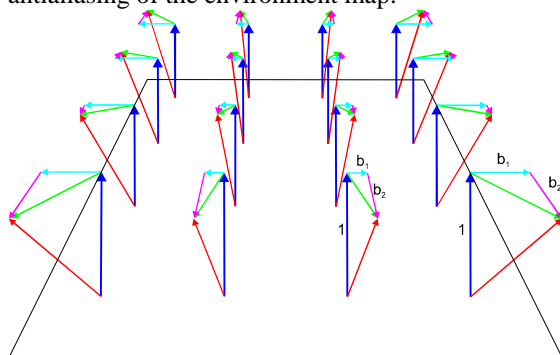


Fig. 4: Representation of bump map with offset vectors.

In this paper, we will first show a practical representation of bump maps, then introduce an anisotropic measure for the roughness, and then show, how resolution pyramids can be calculated and practically stored. We offer a cheap, isotropic and a more expensive anisotropic version for the

bump-roughness pyramid. Examples will illustrate the different methods.

The representation of bump maps.

Bump mapping, even without antialiasing or environment mapping is not commonly used in real-time systems due to its heavy demands on the computing resources. This is partly, because the traditional approach to bump mapping [4] includes the calculation of the derivatives of the bump function.

Bump mapping with Precalculated Derivatives

A possible solution that avoids the calculation of the derivatives of the bump function is to store precalculated derivatives[6][2]. Besides saving the calculation, this has the advantage, that the scaling of bump maps is as simple as the scaling of rgb-textures. If traditional bump maps are scaled with an unknown factor, it is impossible to calculate the derivatives any more. The most difficult problem that remains to be solved is to find an appropriate local coordinate system for each sample point, which consists of the normal vector of the surface in this point and the two tangential directions, for which the derivatives of the bump function have to be calculated (we have the same problem with the traditional representation of the bump maps). Once this coordinate system has been established, the calculation of the new normal vector is performed by adding the offset vector specified by the precalculated derivatives in the local coordinate system to the surface normal.

The Local Coordinate System

In theory, we are free to choose a suitable local coordinate system for the perturbation of the normals by the bump maps. Of course, the data stored in the bump maps is dependent of the chosen coordinate system. Unfortunately, a local coordinate system that ideally fits all needs for bump mapping doesn't exist. But two conditions should at least be met:

- the directions of the axes should be a continuous function of the location.
- the system should allow to map a bump map on any surface of an object (with any orientation), without having to recalculate the whole bump map. (This means for example, that a bump map describing the letters of the alphabet could be used to carve words into a surface regardless of orientation or location of the writing)

In addition, it would be nice, if

- the coordinate system would be orthogonal (which is not necessarily the case for the projection of the u and v axes on the surface;

this is, by the way, a problem with standard bump mapping).

For the description of some possible solutions, we will use a notation similar to that of Blinn [4]: The points of the original patch are given by

$$\mathbf{p} = \begin{pmatrix} x \\ y \\ z \end{pmatrix}, \text{ the partial derivatives are given by}$$

$$\frac{\partial \mathbf{p}}{\partial u} = \mathbf{p}_u = \begin{pmatrix} x_u \\ y_u \\ z_u \end{pmatrix} \text{ and } \mathbf{p}_v, \text{ the surface normal is}$$

thus $\mathbf{n} = \mathbf{p}_u \times \mathbf{p}_v$. The sufficiently small displacement function f (with partial derivatives f_u and f_v) defines a new surface:

$$\mathbf{p}' = \mathbf{p} + f \frac{\mathbf{n}}{|\mathbf{n}|}.$$

The new normal vector in this notation is

$$\mathbf{n}' = \mathbf{n} + f_u \frac{\mathbf{n}}{|\mathbf{n}|} \times \mathbf{p}_v + f_v \mathbf{p}_u \times \frac{\mathbf{n}}{|\mathbf{n}|}.$$

1. The „natural“ system (perpendicular to u-lines, v-lines, n)

$$\text{We define } \mathbf{s}_u = \frac{\mathbf{n}}{|\mathbf{n}|} \times \mathbf{p}_v \text{ and } \mathbf{s}_v = \mathbf{p}_u \times \frac{\mathbf{n}}{|\mathbf{n}|}.$$

We get:

$$\mathbf{n} = \mathbf{p}_u \times \mathbf{p}_v = \mathbf{s}_u \times \mathbf{s}_v \text{ and}$$

$$\mathbf{n}' = \mathbf{n} + f_u \mathbf{s}_u + f_v \mathbf{s}_v$$

The bump map stores f_u and f_v . This is classical bump mapping with possibly non-orthogonal u-v coordinate system and arbitrary $|\mathbf{p}_u|$ and $|\mathbf{p}_v|$.

Accordant to the notion of f as displacement function, the „height“ of the bumps is constant and does not scale with their size in the other dimensions if the map is scaled. If the u-v mapping is continuous and „well behaved“, the first requirement is also fulfilled and it is possible to interpolate \mathbf{s}_u and \mathbf{s}_v linearly across triangles (with perspective correction). An example for a mapping that makes problems is a sphere, if spherical coordinates are used for u and v; at the pole, one coordinate is not unique. If \mathbf{s}_u and \mathbf{s}_v are interpolated, the lengths of \mathbf{s}_u and \mathbf{s}_v should be interpolated separately from the vectors themselves. As the perspective division doesn't change the directions of the vectors but only the lengths, only the lengths need to be corrected; the correction of the direction is performed automatically by choosing appropriately sized vectors at the vertices.

The direct interpolation of two vectors with different lengths would cause the vector to change directions faster close to the end with the shorter vector.

2. The natural system with normalized unit vectors

As pointed out in Blinn's original bump mapping paper [4], we could also want the bump mapping to be scale invariant. For this, the perturbation vector has to scale at the same rate as \mathbf{n} , independent of scales in \mathbf{p} (or \mathbf{s}_u and \mathbf{s}_v). This can lead to geometrically „impossible“ normals, if the object is scaled with different scales in u and v directions, which should therefore be excluded. The best choice for the coordinate system is the same as the previous one, but with normalized lengths of \mathbf{s}_u and \mathbf{s}_v ; thus the interpolation of the lengths can be saved. Again, perspective division is not needed, as it cancels out in the normalization process.

3. An orthonormal system with main direction m

An interesting alternative for the local coordinate system is an orthogonal system, that is derived from the normal vector \mathbf{n} and a main direction \mathbf{m} . The unit vectors \mathbf{e}_1 and \mathbf{e}_2 are perpendicular to \mathbf{n} .

With the help of \mathbf{m} they are defined such, that \mathbf{e}_2 is perpendicular to \mathbf{m} and \mathbf{e}_1 is in the plane of \mathbf{n} and \mathbf{m} [6]. The main direction \mathbf{m} can be e.g. one of \mathbf{p}_u or \mathbf{p}_v (in this case interpolated as above), but it can also be a constant vector for a whole object. A good example is the mapping onto a sphere like e.g. the earth with spherical coordinates. The direction of the axis of the earth would serve as \mathbf{m} and we would get \mathbf{e}_1 pointing always in east-west direction, and \mathbf{e}_2 in south north direction. An important advantage of a constant main direction \mathbf{m} is that besides the normal vector, no other vector needs to be interpolated across triangles. In addition, the coordinate system can be calculated in hardware in the rasterizer/shader and needs not to be calculated at all vertices by a setup process. The calculation of the local coordinate system $\mathbf{n}, \mathbf{e}_1, \mathbf{e}_2$ from the interpolated normal vector \mathbf{n}_I and the main direction \mathbf{m} is performed using the following formula (Fig. 5):

$$\mathbf{n} = \frac{\mathbf{n}_I}{|\mathbf{n}_I|}, \mathbf{e}_1 = \frac{\mathbf{m} \times \mathbf{n}}{|\mathbf{m} \times \mathbf{n}|}, \mathbf{e}_2 = \mathbf{n} \times \mathbf{e}_1.$$

In this way, we get two tangential vectors:

- \mathbf{e}_2 in the plane defined by \mathbf{n} and \mathbf{m} , and
- \mathbf{e}_1 perpendicular to that plane.

If the vectors need not be normalized, we multiply the three vectors by $|\mathbf{n}_I|$ for simpler calculation and get:

$$\mathbf{n}|\mathbf{n}_I| = \mathbf{n}_I, \mathbf{e}_1|\mathbf{n}_I| = \frac{\mathbf{m} \times \mathbf{n}}{|\mathbf{m} \times \mathbf{n}|}|\mathbf{n}_I|,$$

$$\mathbf{e}_2|\mathbf{n}_I| = \mathbf{n}_I \times \mathbf{e}_1.$$

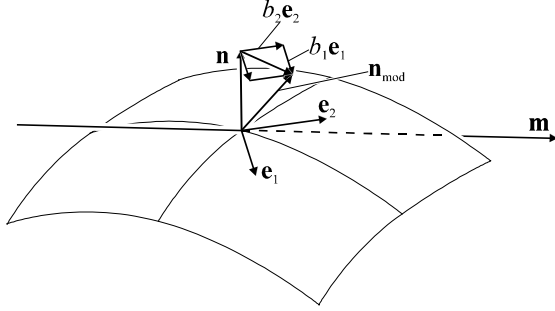


Fig. 5: The construction of the local coordinate system for the bump map using a main direction \mathbf{m} .

The roughness information

We have now defined, how the bump maps can be represented with precalculated derivatives or perturbation vectors in a suitable local coordinate system. The next question is, how to represent the roughness information, i.e. the bumps that are too small to be represented in the current bump map level, but nevertheless are important for the visual appearance of the surface. This roughness information determines ultimately the size and shape of the reflection bodies (Fig. 3), into which the small, pixel-wide viewing beams are reflected by the rough surface. A complete description of the roughness would consist of the complete distribution of perturbation vectors within the considered area. The only difference between the roughness information and the complete detailed bump map is, that the location, where a certain perturbation vector applies, can be omitted. But the complete distribution of perturbation vectors is still much too much information to store and to use. A common way out is to assume a certain form of the distribution, which allows to represent the distribution with only a few parameters. A one-dimensional example for such parameters are average and variance in the case of a normal distribution. The counterpart of the variance in the 2D case is the two-dimensional covariance matrix \mathbf{K} , which describes the distribution in the form of an ellipse: $(\mathbf{x} - \bar{\mathbf{x}})^T \mathbf{K}^{-1} (\mathbf{x} - \bar{\mathbf{x}}) = 1$. On this ellipse, the probability density is constant; the distance of a point \mathbf{x} on the ellipse to the average vector $\bar{\mathbf{x}}$ represents the standard deviation in the direction $(\mathbf{x} - \bar{\mathbf{x}})$ of this point. Of course, the assumption of a normal distribution is not valid in the general case, but the representation of the

roughness with covariance matrices of the perturbation vectors gives us the possibility to represent the normal vector distribution with an elliptical cone, that is characterized by three parameters (plus two for the average direction). This representation is appropriate for most practical normal vector distributions and enables us to model anisotropic reflection effects and produce realistic images of corrugated sheet iron, brushed metal, small scrapes on a glossy surface, waves on a lake and so on.

The calculation of the covariance matrix

The covariance matrix is calculated from the derivatives f_u and f_v in the following way:

$$\mathbf{K} = \frac{1}{n} \begin{bmatrix} \sum_{i=0..n} (f_{u,i} - \bar{f}_u)^2 & \sum_{i=0..n} (f_{u,i} - \bar{f}_u)(f_{v,i} - \bar{f}_v) \\ \sum_{i=0..n} (f_{u,i} - \bar{f}_u)(f_{v,i} - \bar{f}_v) & \sum_{i=0..n} (f_{v,i} - \bar{f}_v)^2 \end{bmatrix} = \begin{bmatrix} a & b \\ b & c \end{bmatrix}$$

This matrix describes an ellipse, shown in Fig. 6 (the one in the middle of the figure). The ellipse

$$\begin{pmatrix} f_u & f_v \end{pmatrix} \mathbf{K}^{-1} \begin{pmatrix} f_u \\ f_v \end{pmatrix} = 1$$

contains about 63% of the perturbation vectors, if their distribution is a two-dimensional normal distribution. If, however, the perturbation vectors $\begin{pmatrix} f_u & f_v \end{pmatrix}$ are equally distributed in a rectangle with edge lengths a and b , the ellipse has the main axes $2a/\sqrt{3}$ and $2b/\sqrt{3}$. We can account for that effect by introducing a correction factor, which we will mention.

We have now the parameters of an ellipse, that describes the distribution of the perturbation vectors and by this the distribution of the normal vectors.

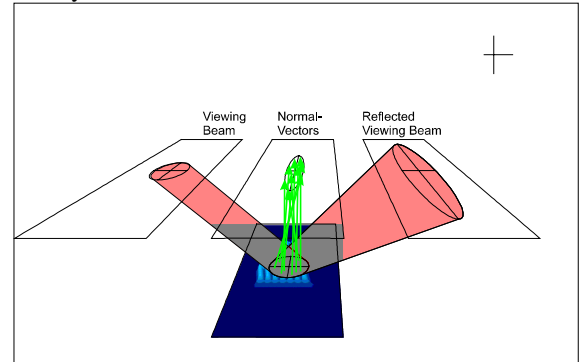


Fig. 6: The viewing rays contributing to a pixel form a beam. This beam is reflected by a bumpy surface into the reflected viewing beam. The shape of the reflected viewing beam is approximated using the distribution of normal vectors in the reflecting area by an elliptical cone. And yes: it

could be argued that the normal vectors that end in the drawn ellipse, should be drawn starting from one origin, not from the surface location, they belong to. The same applies for the reflected beam.

This information can be used in a subsequent step to shade the pixel correctly. Depending on the used shading methods, there exist different possibilities to use the roughness ellipse: In a ray tracer, the ellipse can be used to perform antialiasing by supersampling. A second possibility is to modify the Blinn-Phong shading so that it uses the roughness information (see Appendix A). Of course, it makes no sense to make huge efforts calculating the bump map and then spoil the quality of the result by applying a simple shading model. A method, that leads to a balanced system with high image quality, is to use the roughness information for the anisotropic antialiasing of environment maps [7].

The roughness pyramid

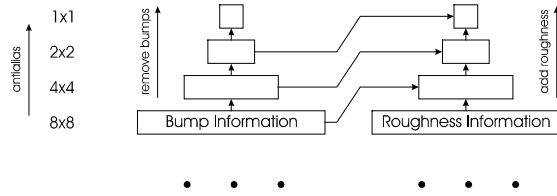


Fig. 7: Bump- and roughness pyramid

Fig. 7 shows, how the surface information is stored in two resolution pyramids, the bump pyramid and the roughness pyramid. The bump pyramid is a standard mip map, its lower resolution levels are calculated by downfiltering the higher resolution levels. In the roughness pyramid, however, the lower resolution levels contain not only the roughness information of the higher resolution roughness levels, but also the roughness information coming from the next level in the bump pyramid, i.e. the roughness information representing those bumps, that are omitted from the bump map in the current bump map level.

This contribution is represented with a covariance matrix, calculated as shown above. It has to be added to the downfiltered covariance matrix from the roughness map. As a result we get the recursive rule for the calculation of the roughness covariance matrix in level l (with a 2×2 -boxfilter for creating the mip-map):

$$\mathbf{K} = \frac{1}{4} \left(\sum_{n=0.3}^{l-1} \mathbf{K}_{l-1,n} \begin{bmatrix} \sum_{n=0.3} (f_{u,n} - \bar{f}_u)^2 & \sum_{n=0.3} (f_{u,n} - \bar{f}_u)(f_{v,n} - \bar{f}_v) \\ \sum_{n=0.3} (f_{u,n} - \bar{f}_u)(f_{v,n} - \bar{f}_v) & \sum_{n=0.3} (f_{v,n} - \bar{f}_v)^2 \end{bmatrix} \right)$$

This formula is equivalent to the calculation of the covariance matrix for all f_u and f_v values in the highest resolution level for the whole area covered by the respective texel in level l .

It is, however, not convenient, to store the covariance matrices themselves in the roughness map. This has two reasons:

- the covariance matrix contains the squares of the standard deviations; to get uniform accuracy over the whole range of standard deviations a value proportional to the standard deviations has to be stored.
- if the roughness information is used for the antialiasing of environment maps, not the covariance matrix \mathbf{K} is needed, but a matrix \mathbf{D} with $\mathbf{D}\mathbf{D}^T = \mathbf{K}$.

We get a favorable representation, if we choose

$$\mathbf{D} = \begin{pmatrix} d_1 & d_2 \\ 0 & d_3 \end{pmatrix}$$

and store the three numbers d_1 , d_2 and d_3 , where d_1 and d_3 can be chosen to be nonnegative.

If $\mathbf{K} = \begin{pmatrix} a & b \\ b & c \end{pmatrix}$, we get:

$$d_1 = \sqrt{a - \frac{b^2}{c}},$$

$$d_2 = \frac{b}{\sqrt{c}}, \text{ and}$$

$$d_3 = \sqrt{c}.$$

Isotropic roughness representation

A more compact roughness representation can be achieved, if we restrict ourselves to isotropic roughness information. Instead of three numbers, we only store one number: the standard deviation of the perturbation vector in the direction of the largest variance. We get this number by diagonalizing the

$$\text{covariance matrix } \mathbf{K} = \mathbf{R} \begin{pmatrix} \lambda_1^2 & 0 \\ 0 & \lambda_2^2 \end{pmatrix} \mathbf{R}^{-1}.$$

The value to be stored in the roughness map is λ_1 with $\lambda_1, \lambda_2 \geq 0$ and $\lambda_1 > \lambda_2$. Thus we get a conservative approximation of the variance of the normal vectors within the considered region of the bump map. For the shading, one choice is again to use λ_1 in a simpler version of the modified Blinn-Phong model (Appendix A). Another possibility is to use λ_1 for the determination of the mipmap level when using environment maps with standard mipmapping, as standard mipmapping allows no anisotropic antialiasing anyway.

Example images



Fig 8: Moon over rectangle; waves are bump mapped; antialiasing with roughness pyramids. Background same as environment map.



Fig. 9: Same as Fig 8; no antialiasing.

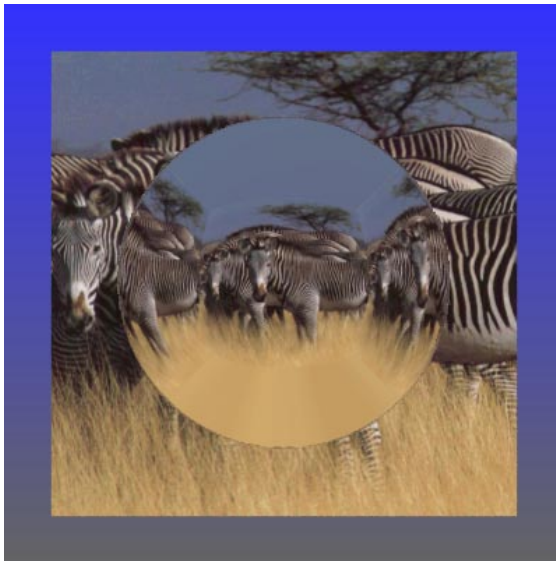


Fig. 10: Reflection of zebras, geometry: flat, with bump map, background: color ramp; environment map: zebras, antialiasing with roughness pyramids.

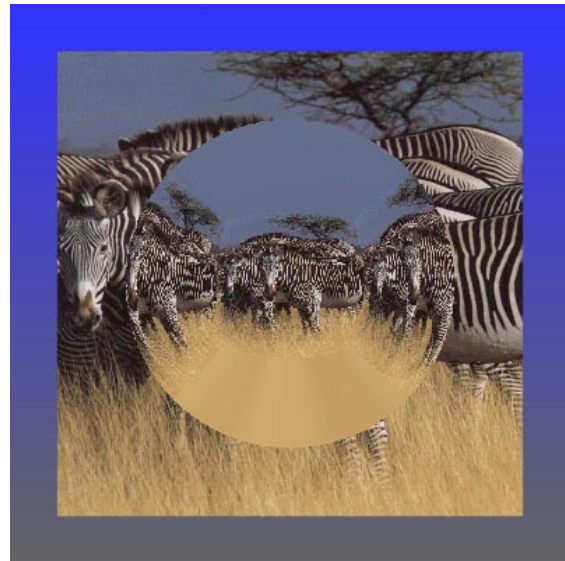


Fig. 11: Same as Fig. 10; no antialiasing

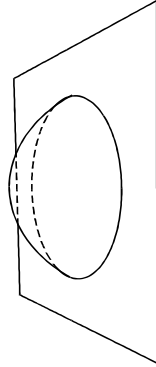


Fig. 12



Fig. 13

Conclusion

We have introduced roughness maps and roughness resolution pyramids as a way to properly antialias bump maps. After mapping color (texture maps) and bumps (bump maps), a new quality of surface properties can now be mapped to objects. Without roughness maps it is quite difficult to render real-looking images of a large class of objects with reasonable effort. Examples are small scratches on glossy surfaces or brushed surfaces but also every kind of bump mapped surface viewed from some distance. The expensive alternative to process such objects would be massive supersampling.

Appendix A: Modified Blinn-Phong Model

In this appendix, we are describing a modification to the Blinn-Phong shading model, that makes use of the roughness information stored in the roughness maps. We are using the Blinn-Phong model (luminance proportional to the dot product of surface normal \mathbf{n} and halfway vector \mathbf{h}) as opposed to the original Phong model (luminance

proportional to the dot product of the reflected light source ray \mathbf{r} and the viewing ray \mathbf{v}). Often the two shading models are regarded as more or less equivalent or at least as having equivalent physical relevance. This is not the case; the Blinn-Phong model is an approximation of a micro-facet model, where the probability to see a facet with normal vector $\mathbf{n}_{micro} = \mathbf{h}$ (for such facets we get reflection of the light source into the eye) is proportional to $(\mathbf{n}^T \mathbf{h})^m$. This is much closer to a physical model than the original Phong model, where the angle between the reflected light ray and the eye vector serves as a measure for the probability to see the reflected light source. This makes no physical sense. In the literature, if a difference between the two methods is recognized, they are compared most often by comparing the form of a highlight on a sphere. For a human observer, the correct form of a highlight on a sphere is difficult to judge. If, however, the form of the highlight on a planar surface would be used, the difference would be obvious (see Fig. 14).

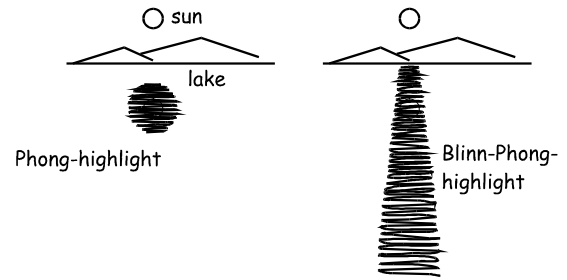


Fig. 14: Phong shading vs. Blinn-Phong shading (outline of PB-highlight plotted with Maple).

The modification of the algorithm consists of using a modified value for the dot product

$\mathbf{n}^T \mathbf{h} = \cos(\alpha)$ before the exponentiation depending on the direction of $\mathbf{n} - \mathbf{h}$. If $\mathbf{n} - \mathbf{h}$ points into the direction of greater variance of \mathbf{n} , the angle is reduced, if the variance of \mathbf{n} in this direction is smaller, it is increased. If \mathbf{d} is the projection of $\mathbf{n} - \mathbf{h}$ into the $\mathbf{e}_1 - \mathbf{e}_2$ -plane, we can modify $\cos(\alpha')$ instead of $\cos(\alpha)$ (see Fig 15 for the geometry used) with:

$$\cos^2(\alpha') = \frac{\cos^2(\alpha)}{|\mathbf{d}|^4 / |\mathbf{Dd}|^2 + \cos^2(\alpha)},$$

where $\cos^2(\alpha) = 1 - |\mathbf{d}|^2$.

We get $\alpha' < \alpha$, if the variance of \mathbf{n} in the regarded direction is larger than 1, otherwise we get $\alpha' \geq \alpha$. If only isotropic roughness information

characterized by λ_1 is used, the formula can be simplified to:

$$\cos^2(\alpha') = \frac{\lambda_1^2 \cos^2(\alpha)}{1 - \cos^2(\alpha) + \lambda_1^2 \cos^2(\alpha)}$$

The size and the decay of the highlight towards its border can still be controlled with the exponent m . However, as the roughness is contained in \mathbf{D} (or λ_1 resp.), it is possible to use a constant exponent m . The size of the highlight is then controlled entirely by the roughness. Another possibility is to use a fixed function $f(\cos^2(\alpha))$ with the desired behavior concerning the decay of the highlight towards its border to calculate the final brightness.

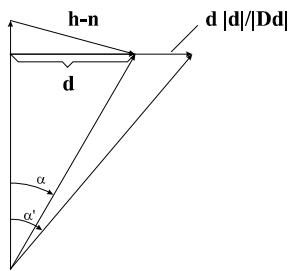


Fig 15: Modification of α with the help of \mathbf{D}

Bibliography

- [1] Becker, B.G., Max, N.L., Smooth Transitions between Bump Rendering Algorithms, Proceedings of SIGGRAPH '93, Computer Graphics 27, Annual Conference Series, pp. 183-190.
- [2] Bennebroek, K., Ernst, I., Rüsseler, H., Wittig, O., Design Principles of Hardware-based Phong Shading and Bump Mapping, in Proceedings of the 11th Eurographics Workshop on Graphics Hardware, Poitiers Aug. 1996.
- [3] Blinn, J., Models of Light Reflection for Computer Synthesized Pictures, SIGGRAPH 77, pp 192-198.
- [4] Blinn, J., Simulation of Wrinkled Surfaces, SIGGRAPH 78, pp 286-292.
- [5] Kirk, D.B., The Simulation of Natural Features Using Cone Tracing, The Visual Computer, vol. 3, no. 2, (August 1987), pp. 63-71.
- [6] Schilling, A., Knittel, G., Straßer, W., Texram: A Smart Memory for Texturing, Computer Graphics & Applications, May 1996, pp. 32-41.
- [7] Schilling, A., Antialiasing of Environment Maps, to be published.